BROOKHAVEN
NATIONAL LABORATORY

BNL-114162-2017-BC

Temperature Dependence in Homogeneous and Heterogeneous Nucleation

R. L. McGraw

Accepted for publication in
Proceedings of the 20th International Conference on Nucleation and Atmospheric Aerosols,
Report Series in Aerosol Science No. 200

August 2017

Environmental & Climate Science Dept.

Brookhaven National Laboratory

U.S. Department of Energy
USDOE Office of Science (SC),
Biological and Environmental Research (BER) (SC-23)

DISCLAIMER

TEMPERATURE DEPENDENCE IN HOMOGENEOUS AND HETEROGENEOUS NUCLEATION

R. L. MCGRAW[1], P. M. WINKLER[2], AND P. E. WAGNER[2]

[1]Environmental and Climate Sciences Department, Brookhaven National Laboratory
Upton, NY, 11973.

[2]Faculty of Physics, University of Vienna, Boltzmanngasse 5, 1090 Vienna, Austria.

Keywords: HETEROGENEOUS NUCLEATION, ATMOSPHERIC NEW PARTICLE FORMATION, NANOPARTICLE WETTING, WETTING PHASE TRANSITION, LINE TENSION

INTRODUCTION

Heterogeneous nucleation on stable (sub-2 nm) nuclei aids the formation of atmospheric cloud condensation nuclei (CCN) by circumventing or reducing vapor pressure barriers that would otherwise limit condensation and new particle growth. Aerosol and cloud formation depend largely on the interaction between a condensing liquid and the nucleating site. A new paper published this year reports the first direct experimental determination of contact angles as well as contact line curvature and other geometric properties of a spherical cap nucleus at nanometer scale using measurements from the Vienna Size Analyzing Nucleus Counter (SANC) (Winkler et al., 2016). For water nucleating heterogeneously on silver oxide nanoparticles we find contact angles around 15 degrees compared to around 90 degrees for the macroscopically measured equilibrium angle for water on bulk silver. The small microscopic contact angles can be attributed via the generalized Young equation to a negative line tension that becomes increasingly dominant with increasing curvature of the contact line. These results enable a consistent theoretical description of heterogeneous nucleation and provide firm insight to the wetting of nanosized objects.

A second paper (McGraw et al. submitted) uses the direct experimental determination approach to examine temperature dependence of heterogeneous nucleation. As in Winkler et al. (2016), which focused on the isothermal case, we again use measurements from the SANC but for fixed seed diameter and over a temperature range (Kupc et al., 2013). Our re-examination of the Kupc et al. measurements uses, first, a model-free theoretic framework, based on the second nucleation theorem (McGraw et al., submitted). The analysis, summarized below, provides a determination of the energy of critical cluster formation directly from the SANC measurements of nucleation probability (c.f. Fig. 1). Temperature dependence is correlated quantitatively through the measurements with stabilization of the water cluster by the silver oxide nanoparticle seed and the findings are used to interpret the unusual temperature dependence found by Kupc et al. (2013) for this system. A necessary condition found here for the observed unusual positive temperature dependence (increasing S_{onset} with increasing temperature T where S_{onset} is the onset value of the water vapor saturation ratio defined more precisely below) is that the critical cluster be more stable on a per molecule basis than the bulk liquid; i.e., the energy lowering through stabilizing molecular interactions between cluster and seed has to more than compensate the positive contribution from surface energy in order to exhibit the effect.

TEMPERATURE DEPENDENCE VIA THE SECOND NUCLEATION THEOREM

The first and second nucleation theorems provide direct microscopic information about the nucleation processes at near molecular scale. Of these the first theorem, which determines molecular number content of the critical nucleus from dependence of the nucleation rate on saturation ratio, is the more commonly used. While both are vital to the analysis, the second nucleation theorem, which infers critical cluster energy from dependence of nucleation rate on temperature (Ford, 1997; McGraw and Wu, 2003), is

central to the present study. For the homogeneous nucleation case where g^* molecules of vapor A_1 combine to form a critical size cluster A_{g^*}:

$$\left(\frac{\partial \ln J_{\text{hom}}}{\partial T}\right)_S = \frac{E_{A_{g^*}} - g^* E_{A_1}^{bulk}}{kT^2} + \frac{E_{A_1} - E_{A_1}^{bulk}}{kT^2}. \tag{1}$$

Here $E_{A_{g^*}}$ is the energy of forming the critical cluster relative to the energy in g^* molecules of bulk liquid each molecule having energy $E_{A_1}^{bulk}$, J_{hom} is the homogeneous nucleation rate per unit volume, S is the vapor saturation ratio and k is the Boltzmann constant. The second term on the right hand side is the energy required to vaporize a single molecule from bulk liquid that emerges from the analysis used to derive Eq. 1 (Ford, 1997).

It is interesting that the bulk liquid reference state enters into consideration of molecular cluster formation from vapor. As shown below this is due to holding $S = n_1 / n_1^{eq}$ constant in the partial derivative, where n_1 is the vapor number concentration and n_1^{eq} its value in equilibrium with bulk liquid. Holding, instead, n_1 constant gives a different result:

$$\left(\frac{\partial \ln J_{\text{hom}}}{\partial T}\right)_{n_1} = \frac{E_{A_{g^*}} - g^* E_{A_1}}{kT^2}, \tag{2}$$

in which the bulk reference state no longer appears. Equations 1 and 2 explain the temperature dependences seen in homogeneous nucleation studies as follows: On a per molecule basis the energies of either the cluster or the vapor exceed the energy of the bulk liquid with the result that the right hand side of Eq. 1 is always positive. Similarly, the energy of the cluster, again on a per-molecule basis, is less than that of the vapor implying that the right hand side of Eq. 2 is always negative. This results in the following inequalities for temperature dependence of the nucleation rate:

$$\left(\frac{\partial \ln J_{\text{hom}}}{\partial T}\right)_S > 0 \tag{3a}$$

$$\left(\frac{\partial \ln J_{\text{hom}}}{\partial T}\right)_{n_1} < 0, \tag{3b}$$

which are in agreement with measurement.

Consider next the heterogeneous nucleation case described at the molecular level by the association reaction:

$$M + n^* A_1 \Leftrightarrow MA_{n^*} \tag{4}$$

where M is a single seed particle and MA_{n^*} is the critical cluster complex. The use of n^* here is to distinguish from the homogeneous case. The analogs to Eqs. 1 and 2 for the heterogeneous case are:

$$\left(\frac{\partial \ln J_1}{\partial T}\right)_S = \frac{E_{MA_{n^*}} - n^* E_{A_1}^{bulk} - E_M}{kT^2} + \frac{E_{A_1} - E_{A_1}^{bulk}}{kT^2} \tag{5a}$$

and

$$\left(\frac{\partial \ln J_1}{\partial T}\right)_{n_1} = \frac{E_{MA_{n^*}} - n^* E_{A_1} - E_M}{kT^2} \tag{5b}$$

respectively. The right hand side of Eq. 5b is always negative, on account that the energy of the associated complex is always less than the sum of energies of the unassociated seed and completely dissociated vapor. For this case, holding n_1 constant in the partial derivative,

$$\left(\frac{\partial \ln J_1}{\partial T}\right)_{n_1} < 0 \tag{6a}$$

and the inequalities for the homogeneous and heterogeneous nucleation cases have the same sign. Equation 5a is more interesting in that the lead term on the right hand side, and thus the whole right hand side, can have either sign:

$$\left(\frac{\partial \ln J_1}{\partial T}\right)_{S} \begin{matrix} > \\ < \end{matrix} 0 \tag{6b}$$

The reason for the ambiguity is that the lead numerator in Eq. 5a reflects the difference in energy between the critical cluster-seed complex and the sum of energies for a free seed particle and n^* molecules of bulk liquid. Sufficiently attractive seed-cluster interactions can overcome the positive surface energy at the cluster-vapor interface so as to make the leading term on the right hand side of Eq. 5a negative, which is the necessary condition for the entire right hand side to be negative, resulting in the unusual (for S held constant in the partial derivative) temperature dependence given by the lower (less than) inequality of Eq. 6b. Sufficiency requires sufficiently attractive seed-cluster interactions to overcome both the cluster surface energy and the vaporization terms that the entire right hand side of Eq. 5a is negative. Otherwise the upper (greater than) inequality of Eq. 6b is maintained and the temperature dependencies are of the same "usual" sign in both the homogeneous and heterogeneous nucleation cases, irrespective of whether the saturation ratio or the number concentration of molecules in the vapor is held constant in the partial derivative.

ANALYSIS OF MEASUREMENTS

The preceding section examined the sensitivity of nucleation rate with respect to temperature and its sign. However, the SANC measurements, (Kupc et al., 2013) and (Schobesberger et al., 2010), don't measure nucleation rate directly but instead measure nucleation probability, as shown for a typical measurement set in Fig. 1. These measurements allow one to determine both the onset saturation ratio, S_{onset}, defined such that $P(S_{onset})$ =1/2, and n^*, which is related to the slope $(dP/dS)_{S=S_{onset}}$ evaluated at S_{onset}. The connection between the per-unactivated-seed nucleation rate, $J_1(S)$ of the previous section (units s^{-1}), and $P(S)$ can be written (McGraw et al., 2012):

$$P(S) = 1 - \frac{N(t_{res})}{N(0)} = 1 - e^{-J_1(S)t_{res}} \tag{7}$$

where $N(t_{res})$ is the concentration of unactivated particles at the residence time t_{res}, defined by the operating conditions of the SANC, and $N(0)$ is the initial seed concentration. From these considerations it follows from Eq. 7 that $J_1(S_{onset})t_{res} = \ln(2)$, which result is used to eliminate the residence time, t_{res}. A convenient expression for $P(S)$, the Gumbel distribution (Gumbel, 1958), derives naturally from the first nucleation theorem applied to the per-seed nucleation rate. The result, which requires no specific model of

the nucleation process, only the fundamental laws of mass action and detailed balance on which the first nucleation theorem itself is based, is the inverse of an equation obtained by Vehkamäki et al (2007) for n^* in terms $P(S)$:

$$P(S) = 1 - \exp\{ -\exp[\ln(\ln 2) + (n^* + 1) (\ln S - \ln S_{onset})] \}. \quad (8)$$

Here n^* follows Eq. 8 as the slope of $P(S)$ evaluated at S_{onset}:

$$\left(\frac{dP}{dS} \right)_{S=S_{onset}} = \frac{(n^* + 1)\ln 2}{2S_{onset}} \quad (9)$$

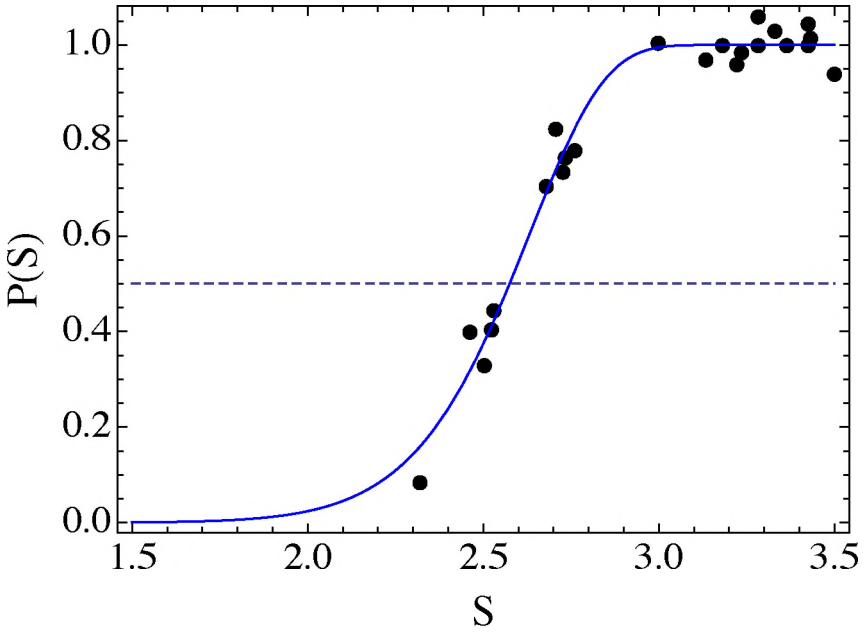

Figure 1: Nucleation probability vs. S for heterogeneous nucleation of water on AgO nanoparticles at 278K. Geometric seed particle diameter = 3.2 nm. Data points, measurements form the Size Analyzing Nucleus Counter (SANC). Dashed line gives the nucleation onset condition $P(S_{onset}) = 0.5$. Curve, Gumbel distribution (Eq. 8) in terms of the two measured parameters S_{onset} and n^* where n^* is the number of water molecules present in the critical seed-cluster complex. Adapted from Winkler et al., 2016.

To make contact with the nucleation probability curves, we examine how S_{onset} , indicated by the point of intersection of the dashed and solid curves in Fig. 1, varies with temperature. The S_{onset} condition maintains a constant per particle nucleation rate. At constant $J_1 = J_1(S_{onset}) = \ln(2) / t_{res}$:

$$d\ln J_1 = (\partial \ln J_1 / \partial T)_{\ln S} dT + (\partial \ln J_1 / \partial \ln S)_T d\ln S = 0 \quad (10)$$

and rearrangement of the second equality gives:

$$(\partial \ln S / \partial T)_{\ln J_1} = -(\partial \ln J_1 / \partial T)_{\ln S} / (\partial \ln J_1 / \partial \ln S)_T \quad (11)$$

The numerator on the right is given by Eq. 5a and the denominator is given in terms of n^* by the first nucleation theorem:

$$(\partial \ln J_1 / \partial \ln S)_T = n^* + 1 . \quad (12)$$

Combining the first and second nucleation theorems from Eqs. 12 and 5a, respectively, with the chain rule, Eq. 11, gives the result we have been seeking (McGraw et al., submitted):

$$\left(\frac{\partial \ln S_{onset}}{\partial T}\right)_{J_1} = -\frac{(E_{MA_{n^*}} - n^* E_{A_1}^{bulk} - E_M) + (E_{A_1} - E_{A_1}^{bulk})}{(n^*+1)kT^2} \tag{13}$$

The measurements of Kupc et al. (2013) show both usual and unusual behavior with a maximum in S_{onset} occurring near 278K as seen in Table 1. This table lists the model-free parameters that can be obtained directly using the methods described in the previous section: n^* follows from Eq. 9 and a parabolic fit to the three measurement points $\{T, \ln S_{onset}\}$ was used to generate estimates for the temperature derivative shown in column 5. These derivatives fix the left hand side of Eq. 13 and are used there together with n^* and the known energy of vaporization from bulk liquid to obtain the energies of formation $\Delta E_f^{hetero} = E_{MA_{n^*}} - n^* E_{A_1}^{bulk} - E_M$ shown in column 6.

r_p (nm) =3.35

$T(K)$	S_{onset}	$\ln S_{onset}$	n^*	$\frac{d \ln S_{onset}}{dT}$	ΔE_f^{hetero} (10^{-20} joule)
274	1.59	0.464	9.7	0.0423	-54.0
278	1.77±0.014	0.571	12.8±0.7	0.0112	-23.6
287	1.43	0.358	12.3	-0.0586	81.6

Table 1. Model-independent parameters S_{onset} and n^* are from fits to the experimental data by Eq. 8. The seed particle size is constant over the set of measurements at geometric radius r_p (nm) =3.35, about twice as large as the seed particles used in the experiment recorded in Fig. 1. Unusual (positive) values of the temperature derivative are seen at lower temperatures followed by transition to normal dependence at higher temperature as indicated by the negative temperature derivative at 287K.

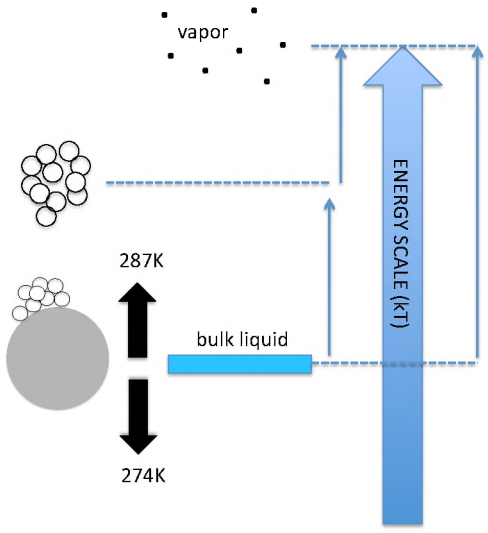

Figure 2. Depiction of critical cluster energies per molecule for homogeneous and heterogeneous nucleation. The positioning of these energies relative to the bulk liquid and vapor reference states determines sign of the temperature dependence.

Figure 2 depicts the disposition of critical cluster energy scales as determined from the present analysis. In homogeneous nucleation, the critical cluster, represented here by the unsupported cluster, always lies intermediate in energy between the vapor and bulk liquid reference states and sign of the temperature dependence (Eqs. 3a and 3b) is unambiguous. For the heterogeneous nucleation case, with special reference to the entries in Table 1, the temperature dependence can have either sign. For clusters lying intermediate in energy between the reference states the sign is normal, i.e. consistent with the homogeneous nucleation case (Eq. 6a) and the upper (greater than) inequality of Eq. 6b, as seen at the higher temperature 287K. At lower temperatures, stabilization of the critical cluster by the seed particle lowers the per-molecule energy below the bulk reference state value, which is the necessary condition for reversal of the sign of the temperature dependence (lower inequality of Eq. 6b) and an increasing S_{onset} with increasing temperature. This unusual temperature dependence occurs in the lower temperature range between 274 and 278K for the series of experiments described in connection with Table 1.

TEMPERATURE DEPENDENCE IN THE FLETCHER MODEL

The model-independent analysis of the preceding section, despite its generality, is somewhat abstract. For this reason it is useful to interpret the general results within the framework of Fletchers classical spherical cap model of the critical cluster in heterogeneous nucleation (Fletcher, 1958). The analysis methods of Winkler et al., 2016, applied to the nucleation probability measurements, enable the direct determination of a unique microscopic contact angle from measured values of S_{onset} and n^*. First, the cap radius of curvature at the liquid-vapor interface, r^* is determined from S_{onset} and the molecular volume and surface tension of water by the Kelvin relation:

$$r^* = \frac{2v_1\sigma_{lv}}{kT\ln S_{onset}} \tag{14}$$

Then from r^*, n^*, and the seed particle radius, r_p, the contact angle θ, which is the key parameter for characterizing seed-cap interactions in the Fletcher model, is uniquely determined (Winkler et al., 2016). Additional microscopic parameters including area of the seed-cap interface Ω_{sl}, the polar angle ϕ, and geodesic curvature of the three-phase contact line (Fig. 3) are also directly determined for use with the spherical cap model (Winkler et al., 2016). Numerical values computed for some of these quantities are given in Table 2. To-scale cross sections of the critical seed-cap assembly are shown in Fig. 4.

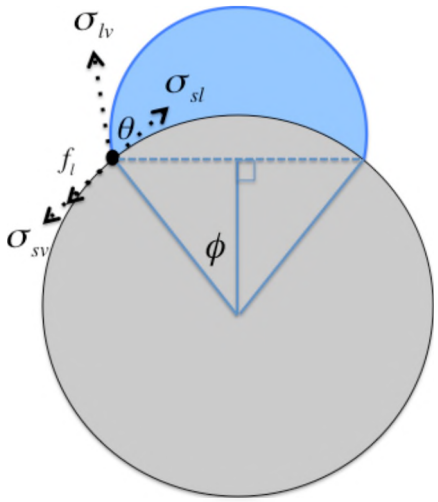

Figure 3. Spherical cap model and notation used in the Fletcher theory. Disposition of the line tension force (not included in the Fletcher model) is also shown.

r_p (nm) =3.35

T(K)	r^*(nm)	θ (deg)	ϕ (deg)	d cos θ/dT	Ω_{sl} (nm^2)	ΔH_w (10^{-20} joule)
274	2.58	7.79	23.8	-0.0046	5.98	-125.
278	2.05	14.7±0.3	20.8	-0.0030	4.61	-79.9
287	3.11	3.14	34.8	0.0029	12.6	-67.7

Table 2. Continuation of Table 1 to include additional parameters derived using the Fletcher model. The critical radius, r^*, results from the measured S_{onset} via Eq. 14 using surface tension and density of water from Wölk and Strey (2001). θ is the directly determined microscopic contact angle and d cos θ /dT its temperature dependence. Ω_{sl} is the seed-cap contact area and ΔH_w is the microscopic heat of wetting (Harkins and Jura, 1944; Neumann, 1974). The necessary condition for unusual temperature dependence in the Fletcher model is that d cos θ /dT < 0, which is satisfied (column 5) over the lower range of temperature as required for consistency with the energy criterion $\Delta E_f^{hetero} < 0$ (Table 1).

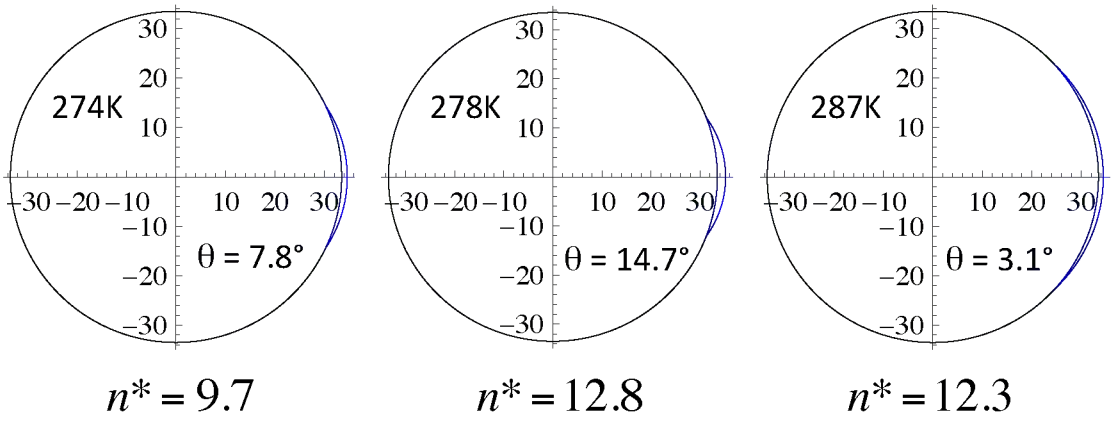

Figure 4. To-scale cross sections of the critical seed-cap assembly constructed using the parameters listed in Table 2 (scale is in angstrom units).

A physical interpretation for the energies derived from the second nucleation theorem analysis is again best achieved using a microphysical model. McGraw et al. (submitted) employ the classical heterogeneous nucleation model of Fletcher for this purpose (Fletcher, 1958). A key step in our calculation of cluster formation energies relative to the bulk liquid looks at the surface work and computes energies through the imaginary process of reversibly extruding the adsorbed critical cluster from bulk liquid phase following the thermodynamic analysis for droplet extrusion introduced by Reiss (1965). The key interaction parameter in the Fletcher model is the contact angle θ, specifically cos(θ). For computing surface energies (rather than free energies) one requires additionally the temperature derivatives for both the liquid-vapor surface tension and θ, specifically d cos(θ)/dT. As with the cluster formation energies, these are obtained from the dependence of S_{onset} on T estimated from the measurements (entries in column 5 of Table 1). Details of the calculations, only summarized here, are given in McGraw et al. (submitted).

A key finding from that work is that the necessary condition for unusual temperature dependence, formulated in the previous sections in terms of seed-cluster interaction energy, has a nice counterpart in terms of the contact angle in the Fletcher theory, namely: $d\cos\theta / dT < 0$, equivalently $d\theta / dT > 0$. This condition, now firmly established theoretically, is consistent with the observation of Schobesberger et al. (2010) of being able to fit the Fletcher model to the unusual temperature dependence that they observed

for n-propanol condensation on NaCl seed particles only by having the contact angle increase with increasing temperature.

ACKNOWLEDGEMENTS

The authors thank Dr. Tamara Pinterich for valuable discussions. RLM was supported by the Atmospheric Systems Research (ASR) Program of the US Department of Energy. PMW and PEW acknowledge support by the European Research Council under the European Community's Seventh Framework Programme (FP7/2007–2013)/ERC grant agreement No. 616075, and the Austrian Science Fund (FWF) (project no. P19546, L593).

REFERENCES

Fletcher, N. H. (1958). Size Effect in Heterogeneous Nucleation. *J. Chem. Phys.* **29**, 572.

Ford, I. J. (1997). Nucleation theorems, the statistical mechanics of molecular clusters, and a revision of classical nucleation theory, *Phys. Rev. E* **56**, 5615.

Gumbel, E. J. (1958), *Statistics of Extremes* (Dover, Mineola, New York) pg. 159.

Harkins, W. D. and G. Jura (1944). Surfaces of Solids. XIII. An absolute method for the determination of the area of a finely divided crystalline solid, *J. Amer. Chem. Soc.* **66**, 1362.

Kupc, A., Winkler, P. M., Vrtala, A. & P. E. Wagner (2013). Unusual Temperature Dependence of Heterogeneous Nucleation of Water Vapor on Ag Particles. *Aerosol Sci. Technol.* **47**, i-iv.

McGraw, R. and D. Wu (2003). Kinetic extensions of the nucleation theorem, *J. Chem. Phys.* **118**, 9337.

McGraw, R., J. Wang & C. Kuang (2012), Kinetics of heterogeneous nucleation in supersaturated vapor: Fundamental limits to neutral particle detection revisited, *Aerosol Sci. Technol.*, **46**, 1053.

Neumann, A. W. (1974). Contact angles and their temperature dependence: Thermodynamic status, measurement, interpretation and application, *Adv. Coll. & Interface Sci.* **4**, 105.

Reiss, H. (1965), *Methods of Thermodynamics* (Dover, Mineola, New York) Chap XI.

Schobesberger, S., P. M. Winkler, T. Pinterich, A. Vrtala, M. Kulmala & P. E. Wagner (2010). Experiments on the temperature dependence of heterogeneous nucleation on nanometer-sized NaCl and Ag particles, *ChemPhysChem* **11**, 3874.

Vehkamäki, H. *et al.* (2007). Heterogeneous multicomponent nucleation theorems for the analysis of nanoclusters. *J. Chem. Phys.* **126**, 174707.

Winkler, P. M., et al. (2016). Direct determination of three-phase contact line properties on nearly molecular scale. *Nature Sci. Rep.* **6**, 26111.

Wölk, J. and R. Strey (2001). Homogeneous nucleation of H_2O and D_2O in comparison: The isotope effect, *J. Phys. Chem. B* **105**, 11683.